JCI The Journal of Clinical Investigation

Inhibition of protein kinase Cε prevents hepatic insulin resistance in nonalcoholic fatty liver disease

Varman T. Samuel, … , Sanjay Bhanot, Gerald I. Shulman

J Clin Invest. 2007;117(3):739-745. https://doi.org/10.1172/JCI30400.

Research Article **Metabolism**

Nonalcoholic fatty liver disease is strongly associated with hepatic insulin resistance and type 2 diabetes mellitus, but the molecular signals linking hepatic fat accumulation to hepatic insulin resistance are unknown. Three days of high-fat feeding in rats results specifically in hepatic steatosis and hepatic insulin resistance. In this setting, PKCε, but not other isoforms of PKC, is activated. To determine whether PKCε plays a causal role in the pathogenesis of hepatic insulin resistance, we treated rats with an antisense oligonucleotide against PKCε and subjected them to 3 days of high-fat feeding. Knocking down PKCε expression protects rats from fat-induced hepatic insulin resistance and reverses fat-induced defects in hepatic insulin signaling. Furthermore, we show that PKCε associates with the insulin receptor in vivo and impairs insulin receptor kinase activity both in vivo and in vitro. These data support the hypothesis that PKCε plays a critical role in mediating fat-induced hepatic insulin resistance and represents a novel therapeutic target for type 2 diabetes.

Inhibition of protein kinase Cε prevents hepatic insulin resistance in nonalcoholic fatty liver disease

Varman T. Samuel,[1,2] Zhen-Xiang Liu,[1] Amy Wang,[1] Sara A. Beddow,[1] John G. Geisler,[3] Mario Kahn,[1] Xian-man Zhang,[1] Brett P. Monia,[3] Sanjay Bhanot,[3] and Gerald I. Shulman[1,4,5]

[1]Department of Internal Medicine, Yale University School of Medicine, New Haven, Connecticut, USA. [2]Veterans Administration Medical Center, West Haven, Connecticut, USA. [3]Isis Pharmaceuticals Inc., Carlsbad, California, USA. [4]Department of Cellular and Molecular Physiology and [5]Howard Hughes Medical Institute, Yale University School of Medicine, New Haven, Connecticut, USA.

Nonalcoholic fatty liver disease is strongly associated with hepatic insulin resistance and type 2 diabetes mellitus, but the molecular signals linking hepatic fat accumulation to hepatic insulin resistance are unknown. Three days of high-fat feeding in rats results specifically in hepatic steatosis and hepatic insulin resistance. In this setting, PKCε, but not other isoforms of PKC, is activated. To determine whether PKCε plays a causal role in the pathogenesis of hepatic insulin resistance, we treated rats with an antisense oligonucleotide against PKCε and subjected them to 3 days of high-fat feeding. Knocking down PKCε expression protects rats from fat-induced hepatic insulin resistance and reverses fat-induced defects in hepatic insulin signaling. Furthermore, we show that PKCε associates with the insulin receptor in vivo and impairs insulin receptor kinase activity both in vivo and in vitro. These data support the hypothesis that PKCε plays a critical role in mediating fat-induced hepatic insulin resistance and represents a novel therapeutic target for type 2 diabetes.

Introduction

Globally, diabetes affects 170 million people, and this number is predicted to increase to over 350 million in the next 25 years (1). Hepatic insulin resistance, a cardinal feature of type 2 diabetes mellitus (T2DM), contributes to both fasting and postprandial hyperglycemia. The cellular mechanisms responsible for causing hepatic insulin resistance remain controversial, with disparate hypotheses attributing causality to visceral fat (2), adipokines (3, 4), ER stress (5), and inflammation (6). An alternate hypothesis is that the development of hepatic steatosis per se causes hepatic insulin resistance. Hepatic steatosis is highly prevalent in patients with type 2 diabetes, and multiple lines of evidence support the role of intrahepatic fat in causing hepatic insulin resistance (7–12). Preventing fat accumulation in rodents preserves hepatic insulin action (7, 10, 12). Amelioration of nonalcoholic fatty liver disease (NAFLD) in patients with T2DM by weight reduction is associated with reversal of hepatic insulin resistance and a return to normoglycemia (9). In this study, we provide a molecular mechanism linking hepatic steatosis to hepatic insulin resistance.

Rats fed a high-fat diet for 3 days develop hepatic steatosis and hepatic insulin resistance in the absence of the confounding effects of peripheral insulin resistance (10, 13). In this setting, activation of PKCε is associated with hepatic insulin resistance. Preventing fat accumulation by inhibiting lipid synthesis via disruption of the mitochondrial acyl-CoA:glycerol-*sn*-3-phosphate acyltransferase (7) or promoting fat oxidation using either the mitochondrial uncoupler 2,4-dinitrophenol (10) or inhibition of acetyl-CoA carboxylase-1 and -2 (12) prevents PKCε activation and hepatic insulin resistance. To determine whether PKCε plays a causal role in the pathogenesis of fat-induced hepatic insulin resistance, we used antisense oligonucleotides (ASOs) against PKCε to decrease translation of PKCε in normal rats. ASOs are avidly taken up by the liver, where they inhibit specific genes of interest. Moreover, ASOs enable knockdown of target genes in normal, mature animals without having to contend with differences in background strain or the effects of genetic manipulation on development and chronic adaptive responses. After 4 weeks of treatment with saline, a control ASO, or PKCε ASO, rats were subjected to 3 days of high-fat feeding, and changes in liver, muscle, and adipose insulin action were assessed by hyperinsulinemic-euglycemic clamping.

Results

PKCε ASO is specific and effective. PKCε ASO treatment specifically reduced *PKCε* expression in liver and white adipose tissue after 4 weeks of treatment at 75 mg/kg per week (Figure 1A). The reduction in mRNA translated into a similar reduction in PKCε protein content relative to that in saline-treated animals (Figure 1B). In contrast, PKCε ASO treatment did not alter muscle PKCε expression. The amount of PKCδ was unchanged by PKCε ASO treatment. ASO treatment was not associated with any adverse events. Specifically, rats remained free of hepatotoxicity, as reflected by the absence of transaminase elevation (aspartate aminotransferase [AST]: saline, 57 ± 0.3; PKCε, 68 ± 3; alanine aminotransferase [ALT]: saline, 76 ± 3; PKCε, 87 ± 5), and exhibited similar weight gain (Figure 1C) across all 3 groups. Finally, there were no differences in plasma concentrations of IL-6 (saline, 150 ± 40 pg/ml; control, 112 ± 34 pg/ml; PKCε, 97 ± 25 pg/ml), leptin (saline, 1,346 ± 274 pg/ml; control, 1,368 ± 223 pg/ml; PKCε, 1,548 ± 225 pg/ml), adiponectin (saline, 21.9 ± 3.2 μg/ml; control, 19.75 ± 3.0 μg/ml; PKCε, 17.6 ± 3.4 μg/ml), or resistin (saline, 26.9 ± 5.7 ng/ml; control, 32.9 ± 6.3 ng/ml; PKCε, 35.7 ± 6.5 ng/ml).

Nonstandard abbreviations used: ASO, antisense oligonucleotide; DAG, diacylglycerol; IRS, insulin receptor substrate; NAFLD, nonalcoholic fatty liver disease; T2DM, type 2 diabetes mellitus.

Conflict of interest: Sanjay Bhanot and Brett P. Monia own stock and/or hold stock options in Isis Pharmaceuticals Inc.

Citation for this article: *J. Clin. Invest.* **117**:739–745 (2007). doi:10.1172/JCI30400.

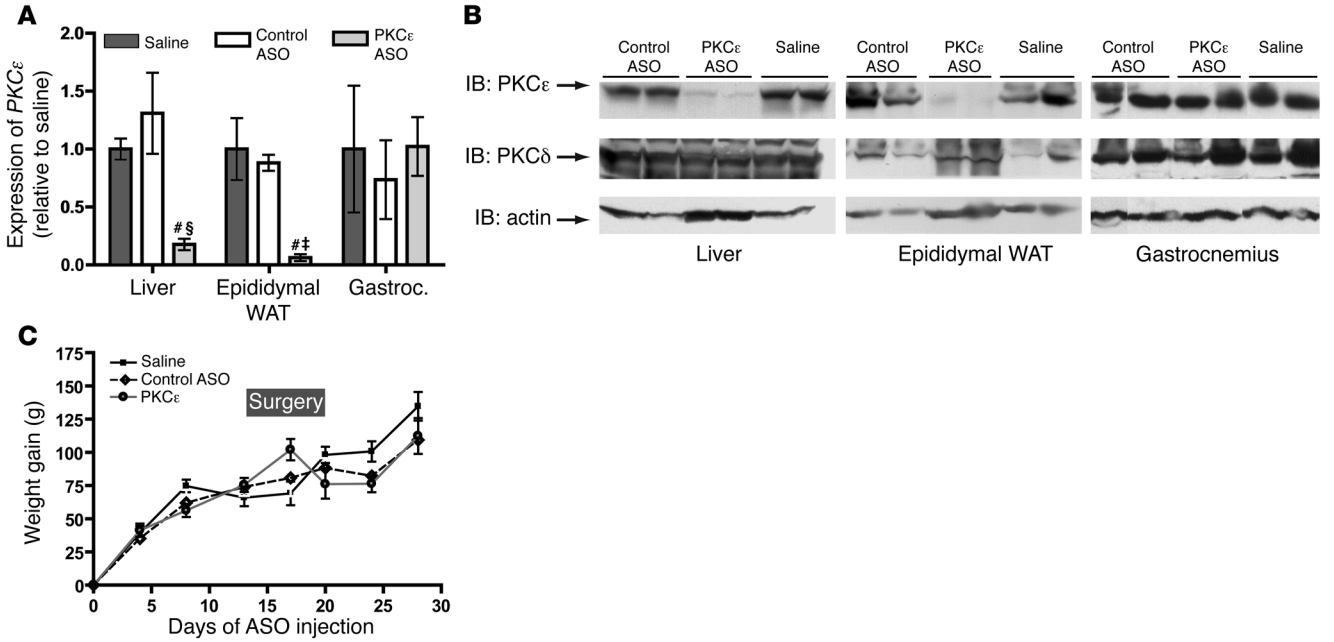

Figure 1

PKCε ASO is effective and well tolerated. (**A**) The amount of *PKC*ε mRNA was determined by quantitative RT-PCR after 4 weeks of treatment with saline, a control ASO, and a specific ASO against PKCε (PKCε ASO). Data are expressed as relative to expression in saline. $^{\#}P < 0.01$ versus saline; $^{\S}P < 0.001$ versus control; $^{\ddagger}P < 0.01$ versus control. (**B**) PKCε ASO specifically decreases PKCε protein levels in liver and epididymal white adipose tissue (WAT), but not in gastrocnemius. (**C**) Weight gain over 4 weeks of ASO therapy. Surgery was performed on rats between days 15 and 20.

PKCε ASO treatment does not alter liver lipids but lowers plasma insulin. Liver triglyceride content and diacylglycerol (DAG) content were similar in all 3 groups (Figure 2, C and D). Fasting plasma fatty acid concentration was also similar across all groups (saline, 0.69 ± 0.11; control, 0.66 ± 0.08; PKCε, 0.59 ± 0.08; ANOVA $P = 0.68$). Though fasting plasma glucose was identical across all 3 groups (Figure 2A), plasma insulin concentration was approximately 50% lower in PKCε ASO–treated rats compared with saline- and control ASO–treated rats (Figure 2B). The lower insulin concentration approaches values seen in rats on regular (low-fat) chow and suggests improved hepatic insulin sensitivity. In order to further understand the mechanism responsible for this reduction in fasting plasma insulin concentration, we performed hyperinsulinemic-euglycemic clamping.

PKCε ASO treatment improves hepatic and adipose insulin action. Basal rates of glucose production under fasted conditions were identical among the 3 groups. Under hyperinsulinemic conditions, suppression of hepatic glucose production was markedly greater in the PKCε group compared with the saline and control ASO groups (Figure 3B). In addition to the changes in hepatic insulin action, there was a modest but significant increase in insulin-stimulated whole-body glucose disposal in the PKCε ASO–treated animals (Figure 3C). Insulin-stimulated peripheral glucose disposal can be largely accounted for by muscle and, to a lesser extent, adipose tissue glucose metabolism. There were no differences in gastrocnemius or soleus ^{14}C-2-deoxyglucose uptake (Figure 3, D and E). However, in the PKCε ASO–treated rats, glucose uptake in the epididymal white adipose tissue increased nearly 2-fold compared with that in saline and control ASO rats (Figure 3F). The augmented adipose insulin sensitivity is corroborated by an increased suppression of plasma fatty acid concentration during the hyperinsulinemic-euglycemic clamping (Figure 3G).

PKCε ASO treatment improves insulin signaling. In order to examine the mechanism for the improved hepatic insulin action, we examined critical components of the insulin signaling pathway: insulin receptor tyrosine phosphorylation, insulin receptor substrate-2 (IRS2) tyrosine phosphorylation, and AKT2 activation under basal and insulin-stimulated conditions. Insulin receptor tyrosine phosphorylation was similarly increased above basal by approximately 50% in all 3 groups. Insulin failed to increase IRS2 tyrosine phosphorylation in high-fat-fed rats treated with saline or control ASO. In contrast, in rats treated with PKCε ASO, insulin increased IRS2 tyrosine phosphorylation approximately 300% above basal (Figure 4B). These differences in IRS2 tyrosine phosphorylation resulted in an approximately 400% increase in insulin-stimulated AKT2 activity, as compared with the approximately 50% increase in the saline and control ASO groups. In adipose tissue, insulin-stimulated AKT2 activity was increased 221% ± 16% in PKCε ASO–treated rats as compared with 32% ± 11% and 23% ± 20% in saline- and control ASO–treated rats.

PKCε interferes with insulin receptor activation. To determine whether PKCε interacts with the insulin receptor in vivo, we performed coimmunoprecipitation experiments. Immunoprecipitation of insulin receptor from liver protein extracts pulled down PKCε, and immunoprecipitation of PKCε also pulled down insulin receptor (Figure 4D). Thus, these 2 proteins bind to each other in vivo. Next, to determine whether the insulin receptor kinase activity was affected by PKCε, we coincubated recombinant active insulin receptor-β with recombinant (active) PKCε. Increasing molar ratios of PKCε to insulin receptor-β resulted in a dose-dependent decrease in insulin receptor-β tyrosine kinase activity, suggesting that PKCε could directly inhibit insulin receptor kinase activity (Figure 4E). Finally, we directly assessed the activity of hepatic insulin receptor kinase

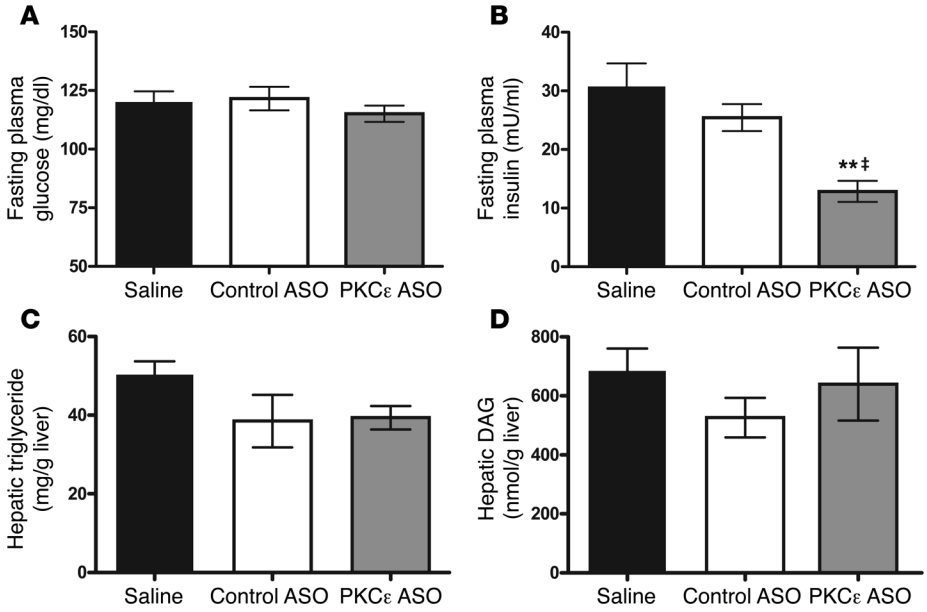

Figure 2
PKCε ASO reduces fasting concentration of insulin without changes in plasma glucose, intrahepatic triglyceride, or DAG. (**A**) Fasting plasma glucose. (**B**) Fasting plasma insulin. $^{**}P < 0.001$ versus saline; $^{‡}P < 0.01$ versus control ASO. (**C**) Hepatic triglyceride content. (**D**) Intrahepatic total DAG.

in rats fed control (low-fat) chow in comparison with high-fat-fed rats treated with saline, control ASO, or PKCε ASO. In comparison with insulin receptor kinase activity in normal rats fed regular chow, the ability of insulin (40 nM) to activate purified receptor in saline-treated high-fat-fed rats was diminished (Figure 4F). The diminished activation was also present in high-fat-fed rats treated with control ASO. In contrast, insulin receptor obtained from PKCε ASO–treated rats had preserved activation of the insulin receptor kinase.

Discussion

NAFLD is strongly linked to hepatic insulin resistance, and T2DM and is now the most common chronic liver disease in the United States (14). We have previously shown that hepatic steatosis results in insulin resistance with the development of fat-induced defects in the insulin signaling pathway. Specifically, the ability of the insulin receptor to tyrosine-phosphorylate its substrates IRS1 and IRS2 is diminished. This proximal defect in the insulin signaling cascade limits the ability of insulin to suppress hepatic glucose production by inhibiting gluconeogenesis and stimulating glycogen synthesis. Moreover, we observed that the development of diet-induced hepatic steatosis was associated with the activation of PKCε (7, 10, 12). The present set of studies was undertaken to ascertain whether or not PKCε plays a causal role in the development of hepatic insulin resistance.

Using ASOs, we can specifically inhibit a gene of interest in adult animals. In this instance, we inhibited PKCε in adult rats and then assessed changes in glucose metabolism after subjecting them to 3 days of high-fat feeding to induce hepatic steatosis and hepatic insulin resistance. Here we establish that decreasing PKCε expression protects against the development of hepatic insulin resistance and improves adipose insulin action by augmenting the activity of the insulin signaling pathway. Furthermore, these studies show that PKCε may induce insulin resistance by directly interfering with the activation of the insulin receptor kinase by insulin.

PKCε ASO specifically inhibits PKCε, without altering the levels of other PKC isoforms. Specifically, there was no change in the abundance of PKCδ, another novel PKC isoform that has been implicated in the development of hepatic insulin resistance after Intralipid infusion (15, 16). In addition, none of the treatments altered liver lipid content (i.e., triglyceride and DAG). This is important since DAG is a known activator of classic and novel isoforms of PKC and DAG concentrations have closely paralleled insulin resistance in other models (7, 12). Thus, in this model system, we specifically inhibit PKCε without altering other PKC isoforms or the concentration of PKC activators.

Neither fasting plasma glucose concentrations nor basal hepatic glucose production rates were affected by PKCε ASO therapy. Despite the lack of differences in these parameters, fasting plasma insulin concentrations were approximately 50% lower in PKCε ASO–treated rats compared with saline- and control ASO–treated rats. The mean insulin concentration in the PKCε rats was similar to that seen in normal rats on a low-fat diet. This observation, in and of itself, suggests that knockdown of PKCε expression improves insulin sensitivity in high-fat fed rats. The results of hyperinsulinemic-euglycemic clamp studies confirm this. Under hyperinsulinemic conditions, suppression of hepatic glucose production was markedly greater in the PKCε group than in the saline and control ASO groups. Moreover, analysis of the insulin signaling pathway demonstrated that insulin signaling was improved in PKCε-treated rats. Whereas the ability of insulin to increase IRS2 tyrosine phosphorylation was blunted in the saline- and control ASO–treated rats, there was a robust increase in IRS2 tyrosine phosphorylation in the PKCε ASO–treated rats. This same pattern of activation was reflected in insulin-stimulated AKT2 activity. Thus, PKCε ASO treatment prevents the defects in insulin signaling that lead to the development of hepatic insulin resistance.

In addition to the improvements in hepatic insulin action, PKCε ASO improved adipose insulin action. Specifically, augmented insulin activation of AKT2 was associated with improved insulin-stimulated glucose uptake. These findings raise the possibility that PKCε may also play a role in adipose insulin action. While PKCε has been shown to be expressed in adipocytes and in 3T3 fibroblasts (17, 18), its role in the adipocyte is uncertain. PKCε expression has been shown to promote differentiation of 3T3 cells

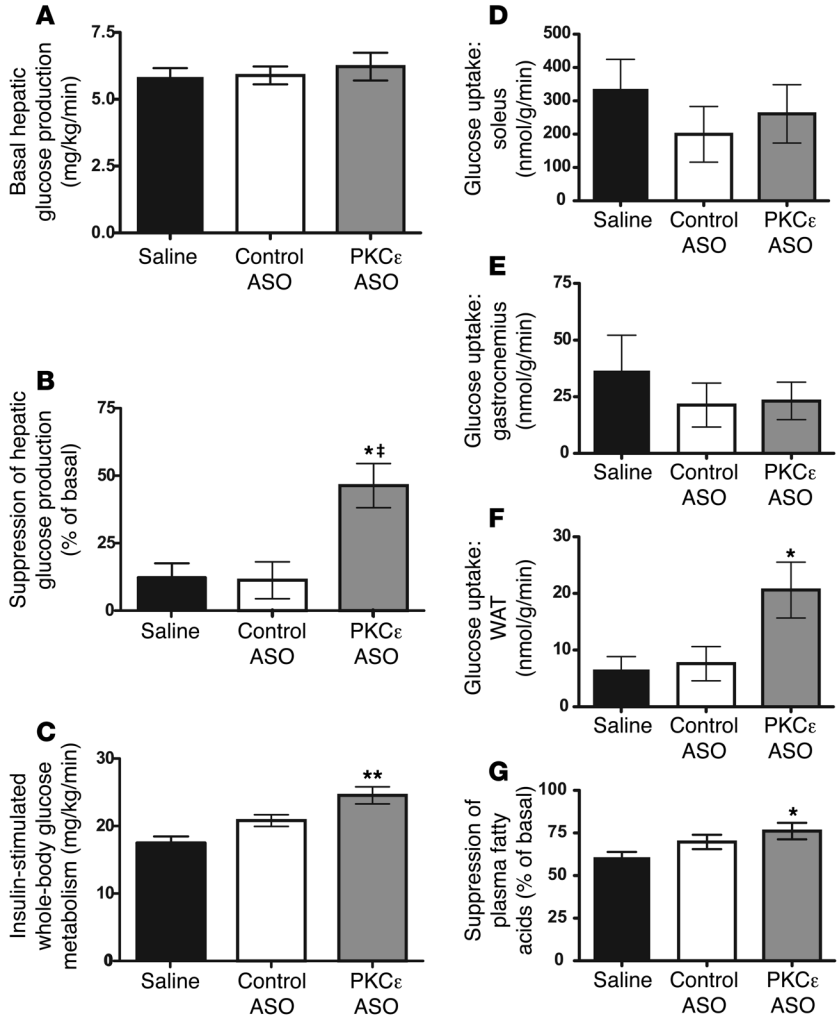

Figure 3
PKCε ASO therapy results in improved hepatic insulin sensitivity and insulin-stimulated adipose glucose uptake. (**A**) Basal rate of endogenous glucose production. (**B**) Percentage suppression of endogenous glucose production during hyperinsulinemic-euglycemic clamping. *$P < 0.05$ versus saline; ‡$P < 0.01$ versus control ASO. (**C**) Rate of insulin-stimulated whole-body glucose uptake. **$P < 0.001$ versus saline. (**D**) Soleus ^{14}C-2-deoxyglucose (2-DOG) uptake. (**E**) Gastrocnemius 2-DOG uptake. (**F**) Epididymal white adipose tissue (WAT) 2-DOG uptake. *$P < 0.05$ versus saline. (**G**) Suppression of plasma fatty acid concentration during hyperinsulinemic-euglycemic clamping. *$P < 0.05$ versus saline.

into adipocytes and increase production of IL-6 (19). However, in the present study, we did not find any significant difference in the concentrations of key adipokines. It is possible that PKCε may directly improve adipose insulin signaling analogously to what we have documented in the liver.

The protective ability of PKCε ASO suggests that PKCε plays a crucial role in the pathogenesis of fat-induced hepatic insulin resistance. Specifically, the finding that decreasing expression of PKCε preserves the ability of the insulin receptor to tyrosine-phosphorylate IRS2 suggests that PKCε interferes with this critical step. Several reports have suggested that insulin resistance may in fact develop from PKC-mediated inhibition of the insulin receptor (20–23). Coghlan and colleagues identified several potential PKC phosphorylation sites on the insulin receptor but failed to detect increased phosphorylation of the insulin receptor in muscle biopsies obtained from diabetic subjects (24, 25). Thus, while PKCs, in general, have been implicated in the pathogenesis of insulin resistance, we delineate the specific role of PKCε in the development of fat-induced hepatic insulin resistance. First, we show here that PKCε and insulin receptor directly associate in vivo, as they each coimmunoprecipitate the other. Second, we demonstrate that incubation of active PKCε with active insulin receptor-β led to a dose-dependent decrease in insulin receptor-β kinase activity, thereby suggesting that PKCε may constrain insulin signaling by hindering the ability of the insulin receptor kinase to tyrosine-phosphorylate its substrates. Finally, we assayed the kinase activity of insulin receptor purified from liver. Insulin activation of insulin receptor kinase activity was diminished in saline- and control ASO–treated high-fat-fed rats as compared with control (low-fat-fed) animals. In comparison, PKCε ASO treatment significantly improved insulin receptor kinase activity. Thus, these data suggest that the diminished tyrosine phosphorylation of IRS2 seen in steatotic livers is a consequence of PKCε-mediated inhibition of the insulin receptor kinase.

Taken together, these data strongly support an important role for PKCε in mediating fat-induced hepatic insulin resistance. On the basis of these results, we hypothesize that fat-induced hepatic insulin resistance arises from DAG-induced activation of PKCε, which directly binds to and inhibits insulin receptor tyrosine kinase activity. A similar mechanism may be present in patients with diabetes; this is supported by Considine et al., who observed activation of PKCε in the livers of obese diabetic patients compared with lean, normoglycemic control subjects (26). Taken together, these data suggest that PKCε inhibition is a novel therapeutic strategy for treatment of hepatic insulin resistance in patients with NAFLD and T2DM.

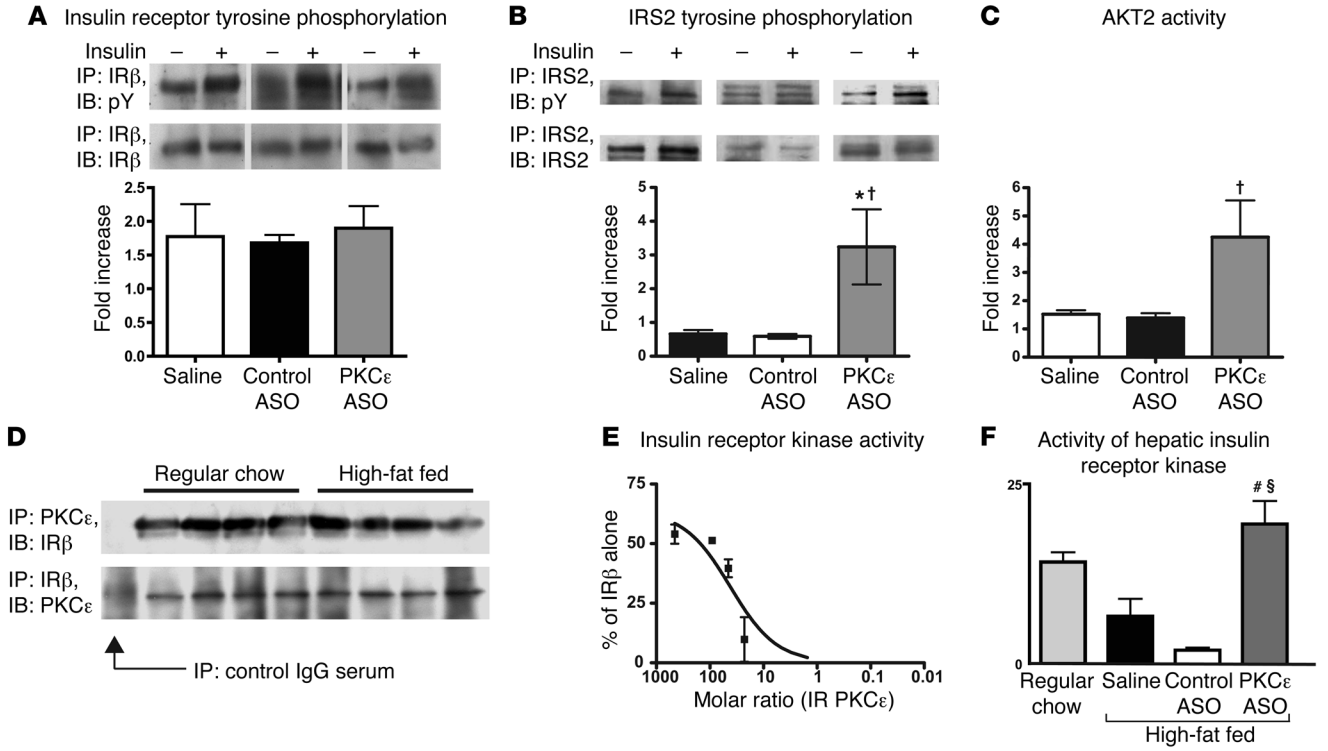

Figure 4
PKCε ASO therapy improves hepatic insulin signaling and preserves insulin receptor kinase activity. Insulin receptor (IR) tyrosine phosphorylation, IRS2 tyrosine phosphorylation, and AKT2 activity were assessed in the basal, fasted state, and after 20 minutes of hyperinsulinemic-euglycemic clamping. (**A**) Insulin receptor tyrosine phosphorylation. (**B**) IRS2 tyrosine phosphorylation. $^{*}P < 0.05$ versus saline; $^{\dagger}P < 0.05$ versus control ASO. (**C**) AKT2 activity. $^{\dagger}P < 0.05$ versus control ASO. (**D**) Immunoprecipitation of the insulin receptor also precipitates PKCε and vice versa. (**E**) Incubation of active insulin receptor kinase with increasing molar ratios of PKCε results in a dose-dependent decrease in insulin receptor kinase activity. (**F**) Activity of lecithin-purified insulin receptor kinase from rats fed a normal low-fat diet and high-fat-fed (HFF) rats treated with saline, control ASO, and PKCε ASO. $^{\#}P < 0.01$ versus HFF/saline; $^{\S}P < 0.001$ versus HFF.

Methods

Animals. The protocols used here were reviewed and approved by the Institutional Animal Care and Use Committee of Yale University School of Medicine. Healthy male Sprague-Dawley rats weighing approximately 250 g were obtained from Charles River Laboratories and acclimated for 1 week after arrival before initiation of the experiment. Rats received food and water ad libitum and were maintained on a 12:12–hour light/dark cycle (lights on at 6:30 am). All ASOs (control and PKCε) were prepared in normal saline, and the solutions were sterilized through a 0.2-μm filter. Rats were dosed with ASO solutions or saline twice per week via i.p. injection at a dose of 75 mg/kg per week for 4 weeks. During the treatment period, body weight and food intake were measured twice weekly. After 14–20 days of ASO treatment, rats underwent the placement of jugular venous and carotid artery catheters. They recovered their presurgical weights by 5–7 days after the operation. After 4 weeks of ASO treatment, rats received a high-fat diet (26% carbohydrate, 59% fat, and 15% protein calories). Safflower oil was the major constituent of the high-fat diet (Dyets Inc.). We and others have previously shown that this diet produces hepatic steatosis and hepatic insulin resistance within 3 days (10, 13).

Selection of rat PKCε ASO. To identify rat PKCε inhibitors, rapid-throughput screens were performed in vitro as previously described (27). In brief, 80 ASOs were designed to the PKCε mRNA sequence, and initial screens identified several potent and specific ASOs, all of which targeted a binding site within the coding region of the PKCε mRNA. After extensive dose-response characterization, the most potent ASO from the screen was chosen: ISIS-232697, with the following sequence: 5′-GCCAGCTCGATCTTGCGCCC-3′. The control ASO, ISIS-141923, has the sequence 5′-CCTTCCCTGAAGGTTCCTCC-3′ and does not have perfect complementarity to any known gene in public databases. The first 5 bases and last 5 bases of chimeric ASOs have a 2′-*O*-(2-methoxy)-ethyl (2′-MOE) modification, and the ASOs also have a phosphorothioate backbone. This chimeric design has been shown to provide both increased nuclease resistance and mRNA affinity, while maintaining the robust RNase H terminating mechanism used by these types of ASOs (28). These benefits result in an attractive in vivo pharmacological and toxicological profile for 2′-MOE chimeric ASOs.

Hyperinsulinemic-euglycemic clamp studies. After 3 days of high-fat feeding, rats were fasted overnight. The following morning, the clamp study began with a prime (1 mg/kg over 10 minutes) of [6,6-^{2}H]glucose followed by a continuous infusion at a rate of 0.1 mg/kg per minute for 2 hours to assess the basal glucose turnover. After the basal period, the hyperinsulinemic-euglycemic clamping was conducted for 120 minutes with a primed/continuous infusion of human insulin (400 mU/kg prime over 10 minutes, 4 mU/kg per minute infusion) (Novo Nordisk) and a variable infusion of 20% dextrose to maintain euglycemia (approximately 100 mg/dl). The 20% glucose was enriched with [6,6-^{2}H]glucose to approximately 2.5% to match the enrichment in the plasma achieved after the basal period. A 25-μCi bolus of 2-deoxy-D-[1-^{14}C]glucose (PerkinElmer) was injected 90 minutes into the clamp to estimate the rate of insulin-stimulated tissue glucose uptake. Additional blood samples (20–60 μl) were taken at 0, 70, and 135 minutes for the determination of plasma fatty acid and insulin con-

centrations. At the end of the clamping, rats were anesthetized with pentobarbital sodium injection (150 mg/kg), and all tissues were taken within 4 minutes, frozen immediately with the use of liquid N_2–cooled aluminum tongs, and stored at –80°C for subsequent analysis.

Biochemical analysis and calculations. Plasma glucose was analyzed during the clamping with the use of 10 μl plasma by a glucose oxidase method on a Beckman Glucose Analyzer II (Beckman Coulter). Plasma insulin, adiponectin, and resistin were measured by RIA using kits from Linco. Plasma leptin and IL-6 were measured using the LINCO*plex* Assay system (Linco). Plasma fatty acid concentrations were determined using an acyl-CoA oxidase–based colorimetric kit (Wako). To determine the enrichment of [6,6-^{2}H]glucose in plasma, samples were deproteinized with 5 volumes of 100% methanol, dried, and derivatized with 1:1 acetic anhydride/pyridine to produce the pentacetate derivative of glucose. The atom percentage enrichment of glucose$_{M+6}$ was then measured by gas chromatographic/mass spectrometric analysis using a Hewlett-Packard 5890 gas chromatograph interfaced to a Hewlett-Packard 5971A mass-selective detector operating in the electron ionization mode (29). Glucose$_{M+2}$ enrichment was determined from the *m/z* ratio 202:200. Rates of basal and insulin-stimulated whole-body glucose turnover were determined as the ratio of the rate of [6,6-^{2}H]glucose infusion (mg/kg per min) to the atom percentage excess glucose$_{M+2}$ (%) in the plasma. This rate was corrected by subtraction of the rate of [6,6-^{2}H]glucose infusion. Hepatic glucose production was determined by subtraction of the glucose infusion rate from the rate of total glucose appearance. For the determination of muscle ^{14}C-2-deoxyglucose-6-phosphate content, muscle samples were homogenized, and the supernatants were subjected to an ion-exchange column to separate ^{14}C-2-deoxyglucose-6-phosphate from 2-deoxyglucose as previously described (30).

Tissue lipid measurement. The DAG extraction and analysis were performed as previously described (31). After purification, DAG fractions were dissolved in methanol/H_2O (1:1, vol/vol) and subjected to liquid chromatography-tandem mass spectrometry (LC/MS/MS) analysis. A Turbo Ion Spray source was interfaced with an API 3000 Tandem Mass Spectrometer (Applied Biosystems) in conjunction with 2 PerkinElmer Series 200 Micro Pumps and a PerkinElmer Series 200 Autosampler. Total DAG content is expressed as the sum of individual species. Tissue triglyceride was extracted by the method of Bligh and Dyer (32) and measured with the use of a DCL Triglyceride Reagent (Diagnostic Chemicals Ltd.).

Insulin signaling. A separate group of rats was used to assess the impact of hepatic fat accumulation on the insulin signaling pathway. These rats were treated exactly as described above and underwent 20 minutes of hyperinsulinemic-euglycemic clamping without a basal infusion. Tissues were harvested in situ immediately at the end of the clamping. Insulin receptor tyrosine phosphorylation was assessed by immunoprecipitation of the insulin receptor with a specific antibody from liver protein extracts and assessment of phosphotyrosine by Western blotting. Similarly, IRS2 tyrosine phosphorylation was assessed by blotting against phosphotyrosine on blots of IRS2 immunoprecipitates. AKT2 activity was assessed from immunoprecipitates by measurement of ^{32}P incorporation onto a synthetic AKT substrate. Assays were performed according to methods previously described (31, 33). For PKC quantification, protein extracts were resolved by SDS-PAGE using 8% gel and electroblotted onto PVDF membrane (DuPont) with the use of a Semi-Dry transfer cell (Bio-Rad). The membrane was then blocked for 2 hours at room temperature in PBS-Tween (10 mmol/l NaH_2PO_4, 80 mmol/l Na_2HPO_4, 0.145 mol/l NaCl, and 0.1% Tween-20, pH 7.4) containing 5% (wt/vol) nonfat dried milk, washed twice, and then incubated overnight with rabbit anti-peptide antibody against PKCε or PKCδ (Santa Cruz Biotechnology Inc.) diluted 1:100 in rinsing solution. After further washings, membranes were incubated with HRP-conjugated IgG fraction of goat anti-rabbit IgG (Bio-Rad), diluted 1:5,000 in PBS-Tween, for 2 hours. These blots were stripped and reblotted with rabbit anti-actin IgG to normalize for variations in protein loading. Blots were scanned and analyzed with ImageJ (NIH).

Insulin activity assay. Insulin receptor was purified from liver homogenates as previously described (34). Briefly, liver samples were homogenized in lysis buffer (50 mM HEPES, 150 mM NaCl, 1 mM EDTA, 0.2 mM Na_3VO_4, 10 mM $Na_4P_2O_7$, 100 mM NaF, 1% Triton X-100, 2 mM phenylmethylsulphonyl fluoride, 10 μg/ml aprotinin, and 1 μg/ml leupeptin). After centrifugation to remove cellular debris, lysates were passed over a wheat-germ agglutinin (Vector Laboratories) column and washed extensively. The insulin receptor was eluted with 0.3 M *N*-acetylglucosamine. The protein was then quantitated, and equal amounts were used for insulin receptor assay against a synthetic substrate, Axltide (Millipore), according to the manufacturer's directions. Similar conditions were used for experiments in which recombinant active PKCε was incubated with recombinant active insulin receptor.

Total RNA preparation and real-time quantitative RT-PCR analysis. Total RNA was extracted from liver samples using the RNeasy kit (QIAGEN). RNA was reverse-transcribed into cDNA with the use of StrataScript Reverse Transcriptase (Stratagene). The abundance of transcripts was assessed by real-time PCR on an Opticon 2 (Bio-Rad) with a SYBR Green detection system (Stratagene). For each run, samples were run in duplicate for both the gene of interest and actin. The expression data for each gene of interest and actin were normalized for the efficiency of amplification, as determined by a standard curve included on each run (35).

Statistics. Values are expressed as mean ± SEM. The significance of the differences in mean values among different treatment groups was evaluated by 1-way ANOVA, followed by post hoc analysis using the Tukey's Honestly Significant Differences (HSD) test. *P* values less than 0.05 were considered significant. All statistical analyses were done with GraphPad Prism 4 (GraphPad Software).

Acknowledgments

We thank Jiaying Dong and Yanna Kosover for expert technical assistance with the studies. We also thank Aida Groszmann for performing the hormone assays. This work was supported by grants from the United States Public Health Service (R01 DK40936 and P30 DK45735 to G.I. Shulman, K23 RR17404 to V.T. Samuel) and a Distinguished Clinical Scientist Award from the American Diabetes Association. G.I. Shulman is an investigator of the Howard Hughes Medical Institute. V.T. Samuel also receives support from the Veterans Administration Medical Center, West Haven, Connecticut, USA.

Received for publication September 20, 2006, and accepted in revised form January 3, 2007.

Address correspondence to: Gerald I. Shulman, TAC S269, PO Box 9812, Yale University School of Medicine, New Haven, Connecticut 06536, USA. Phone: (203) 785-5447; Fax: (203) 737-4059; E-mail: gerald.shulman@yale.edu.

1. Wild, S.H., Roglic, G., Green, A., Sicree, R., and King, H. 2004. Global prevalence of diabetes: estimates for the year 2000 and projections for 2030. Response to Rathman and Giani. *Diabetes Care.* **27**:2569–2570.
2. Kabir, M., et al. 2005. Molecular evidence supporting the portal theory: a causative link between visceral adiposity and hepatic insulin resistance. *Am. J. Physiol. Endocrinol. Metab.* **288**:E454–E461.
3. Kadowaki, T., et al. 2006. Adiponectin and adiponectin receptors in insulin resistance, diabetes, and the metabolic syndrome. *J. Clin. Invest.* **116**:1784–1792. doi:10.1172/JCI29126.
4. Banerjee, R.R., et al. 2004. Regulation of fasted blood glucose by resistin. *Science.* **303**:1195–1198.

5. Ozcan, U., et al. 2006. Chemical chaperones reduce ER stress and restore glucose homeostasis in a mouse model of type 2 diabetes. *Science.* **313**:1137–1140.
6. Shoelson, S.E., Lee, J., and Goldfine, A.B. 2006. Inflammation and insulin resistance. *J. Clin. Invest.* **116**:1793–1801. doi:10.1172/JCI29069.
7. Neschen, S., et al. 2005. Prevention of hepatic steatosis and hepatic insulin resistance in mitochondrial acyl-CoA:glycerol-sn-3-phosphate acyltransferase 1 knockout mice. *Cell Metab.* **2**:55–65.
8. Petersen, K.F., et al. 2002. Leptin reverses insulin resistance and hepatic steatosis in patients with severe lipodystrophy. *J. Clin. Invest.* **109**:1345–1350. doi:10.1172/JCI200215001.
9. Petersen, K.F., et al. 2005. Reversal of nonalcoholic hepatic steatosis, hepatic insulin resistance, and hyperglycemia by moderate weight reduction in patients with type 2 diabetes. *Diabetes.* **54**:603–608.
10. Samuel, V.T., et al. 2004. Mechanism of hepatic insulin resistance in non-alcoholic fatty liver disease. *J. Biol. Chem.* **279**:32345–32353.
11. Kim, J.K., et al. 2001. Tissue-specific overexpression of lipoprotein lipase causes tissue-specific insulin resistance. *Proc. Natl. Acad. Sci. U. S. A.* **98**:7522–7527.
12. Savage, D.B., et al. 2006. Reversal of diet-induced hepatic steatosis and hepatic insulin resistance by antisense oligonucleotide inhibitors of acetyl-CoA carboxylases 1 and 2. *J. Clin. Invest.* **116**:817–824. doi:10.1172/JCI27300.
13. Kraegen, E.W., et al. 1991. Development of muscle insulin resistance after liver insulin resistance in high-fat-fed rats. *Diabetes.* **40**:1397–1403.
14. McCullough, A.J. 2004. The clinical features, diagnosis and natural history of nonalcoholic fatty liver disease. *Clin. Liver Dis.* **8**:521–533, viii.
15. Lam, T.K., et al. 2002. Free fatty acid-induced hepatic insulin resistance: a potential role for protein kinase C-delta. *Am. J. Physiol. Endocrinol. Metab.* **283**:E682–E691.
16. Boden, G., et al. 2005. Free fatty acids produce insulin resistance and activate the proinflammatory nuclear factor-κB pathway in rat liver. *Diabetes.* **54**:3458–3465.
17. Frevert, E.U., and Kahn, B.B. 1996. Protein kinase C isoforms epsilon, eta, delta and zeta in murine adipocytes: expression, subcellular localization and tissue-specific regulation in insulin-resistant states. *Biochem. J.* **316**:865–871.
18. Webb, P.R., Doyle, C., and Anderson, N.G. 2003. Protein kinase C-epsilon promotes adipogenic commitment and is essential for terminal differentiation of 3T3-F442A preadipocytes. *Cell. Mol. Life Sci.* **60**:1504–1512.
19. Ohashi, K., Kanazawa, A., Tsukada, S., and Maeda, S. 2005. PKCepsilon induces interleukin-6 expression through the MAPK pathway in 3T3-L1 adipocytes. *Biochem. Biophys. Res. Commun.* **327**:707–712.
20. Takayama, S., White, M.F., and Kahn, C.R. 1988. Phorbol ester-induced serine phosphorylation of the insulin receptor decreases its tyrosine kinase activity. *J. Biol. Chem.* **263**:3440–3447.
21. Lewis, R.E., Cao, L., Perregaux, D., and Czech, M.P. 1990. Threonine 1336 of the human insulin receptor is a major target for phosphorylation by protein kinase C. *Biochemistry.* **29**:1807–1813.
22. Anderson, C.M., and Olefsky, J.M. 1991. Phorbol ester-mediated protein kinase C interaction with wild-type and COOH-terminal truncated insulin receptors. *J. Biol. Chem.* **266**:21760–21764.
23. Pillay, T.S., Xiao, S., Keranen, L., and Olefsky, J.M. 2004. Regulation of the insulin receptor by protein kinase C isoenzymes: preferential interaction with beta isoenzymes and interaction with the catalytic domain of betaII. *Cell. Signal.* **16**:97–104.
24. Kellerer, M., et al. 1995. Mechanism of insulin receptor kinase inhibition in non–insulin-dependent diabetes mellitus patients. Phosphorylation of serine 1327 or threonine 1348 is unaltered. *J. Clin. Invest.* **96**:6–11.
25. Coghlan, M.P., Pillay, T.S., Tavare, J.M., and Siddle, K. 1994. Site-specific anti-phosphopeptide antibodies: use in assessing insulin receptor serine/threonine phosphorylation state and identification of serine-1327 as a novel site of phorbol ester-induced phosphorylation. *Biochem. J.* **303**:893–899.
26. Considine, R.V., et al. 1995. Protein kinase C is increased in the liver of humans and rats with non–insulin-dependent diabetes mellitus: an alteration not due to hyperglycemia. *J. Clin. Invest.* **95**:2938–2944.
27. Qu, X., Seale, J.P., and Donnelly, R. 1999. Tissue and isoform-selective activation of protein kinase C in insulin-resistant obese Zucker rats: effects of feeding. *J. Endocrinol.* **162**:207–214.
28. Graham, M.J., et al. 1998. In vivo distribution and metabolism of a phosphorothioate oligonucleotide within rat liver after intravenous administration. *J. Pharmacol. Exp. Ther.* **286**:447–458.
29. Hundal, R.S., et al. 2002. Mechanism by which high-dose aspirin improves glucose metabolism in type 2 diabetes. *J. Clin. Invest.* **109**:1321–1326. doi:10.1172/JCI200214955.
30. Youn, J.H., and Buchanan, T.A. 1993. Fasting does not impair insulin-stimulated glucose uptake but alters intracellular glucose metabolism in conscious rats. *Diabetes.* **42**:757–763.
31. Yu, C., et al. 2002. Mechanism by which fatty acids inhibit insulin activation of insulin receptor substrate-1 (IRS-1)–associated phosphatidylinositol 3-kinase activity in muscle. *J. Biol. Chem.* **277**:50230–50236.
32. Bligh, E.G., and Dyer, W.J. 1959. A rapid method of total lipid extraction and purification. *Can. J. Biochem. Physiol.* **37**:911–917.
33. Alessi, D.R., Caudwell, F.B., Andjelkovic, M., Hemmings, B.A., and Cohen, P. 1996. Molecular basis for the substrate specificity of protein kinase B: comparison with MAPKAP kinase-1 and p70 S6 kinase. *FEBS Lett.* **399**:333–338.
34. Kasuga, M., Fujita-Yamaguchi, Y., Blithe, D.L., White, M.F., and Kahn, C.R. 1983. Characterization of the insulin receptor kinase purified from human placental membranes. *J. Biol. Chem.* **258**:10973–10980.
35. Pfaffl, M.W. 2001. A new mathematical model for relative quantification in real-time RT-PCR. *Nucleic Acids Res.* **29**:e45.